

A

		Eukaryotes												
		Opisthokonta												
		Bilateria												
		Mammals												
Genes		Excavata	SAR	Archeplastide	Amoebozoa	Fungi	Cnidaria	Protostomia	Osteichthyes	Amphibian	Sauropsida	Monotremes	Marsupials	Eutherians
<i>Lrrc23</i>		Green	Green	Yellow	Yellow	Yellow	Yellow	Green	Green	Green	Green	Green	Green	Green

B

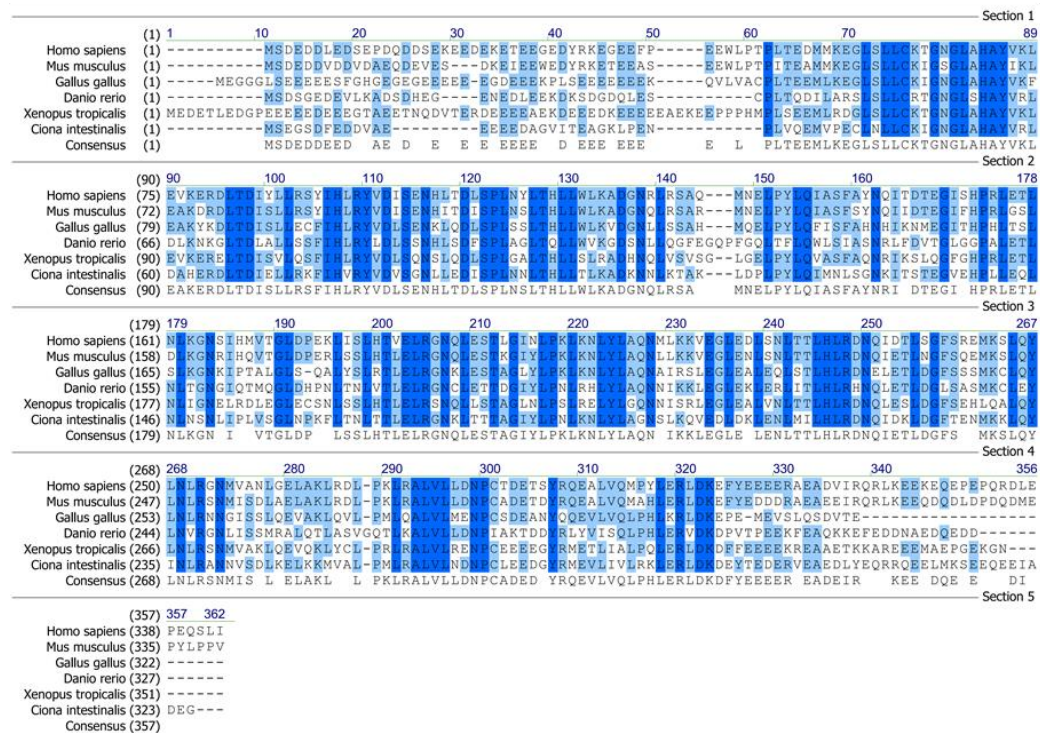


Fig. S1. *Lrrc23* is an evolutionarily conserved gene. (A) *Lrrc23* is present in the most of eukaryotes that utilize flagella (SAR: stramenopiles, alveolates, Rhizaria). Green denotes *Lrrc23* by the most of species within the indicated taxon, whereas yellow indicates a loss of this gene within several species within the indicated taxon. (B) LRRC23 protein sequence similarity across species, with dark blue corresponding to total conservation and light blue indicating conservation among three to five species.

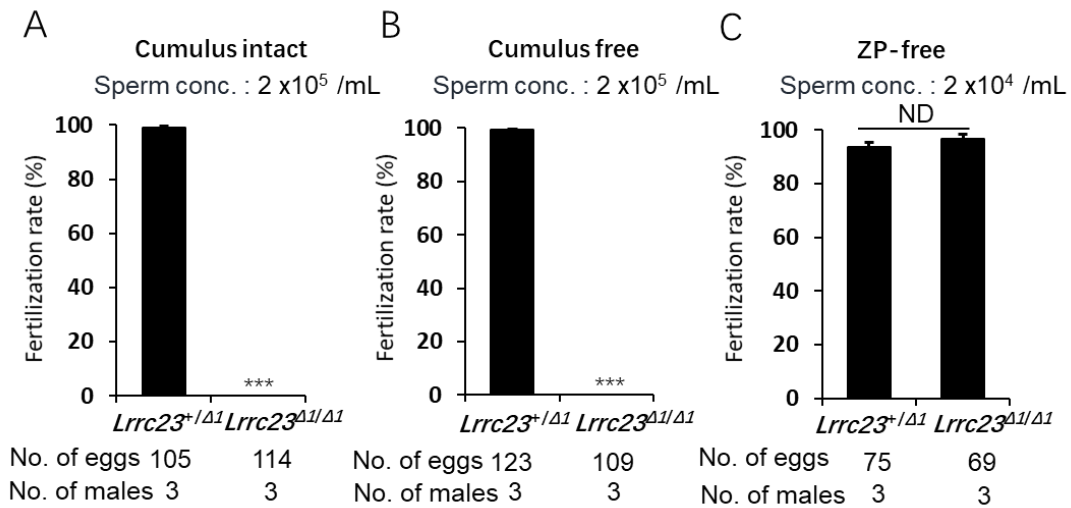


Fig. S2. Assessment of the fertility of spermatozoa from *Lrrc23*^{Δ1/Δ1} mice. (A) Fertilization rates (percentages of two pronuclei [2PN] eggs) in cumulus-intact oocytes inseminated with spermatozoa from *Lrrc23*^{+/Δ1} and *Lrrc23*^{Δ1/Δ1} mice, N = 3, ***P < 0.001. (B) Fertilization rates in cumulus-free oocytes generated with spermatozoa from *Lrrc23*^{+/Δ1} and *Lrrc23*^{Δ1/Δ1} mice, N = 3, ***P < 0.001. (C) Fertilization rates in ZP-free oocytes generated with spermatozoa from *Lrrc23*^{+/Δ1} and *Lrrc23*^{Δ1/Δ1} mice, N = 3, P > 0.05. Error bars represent S.D. Student's t-test.

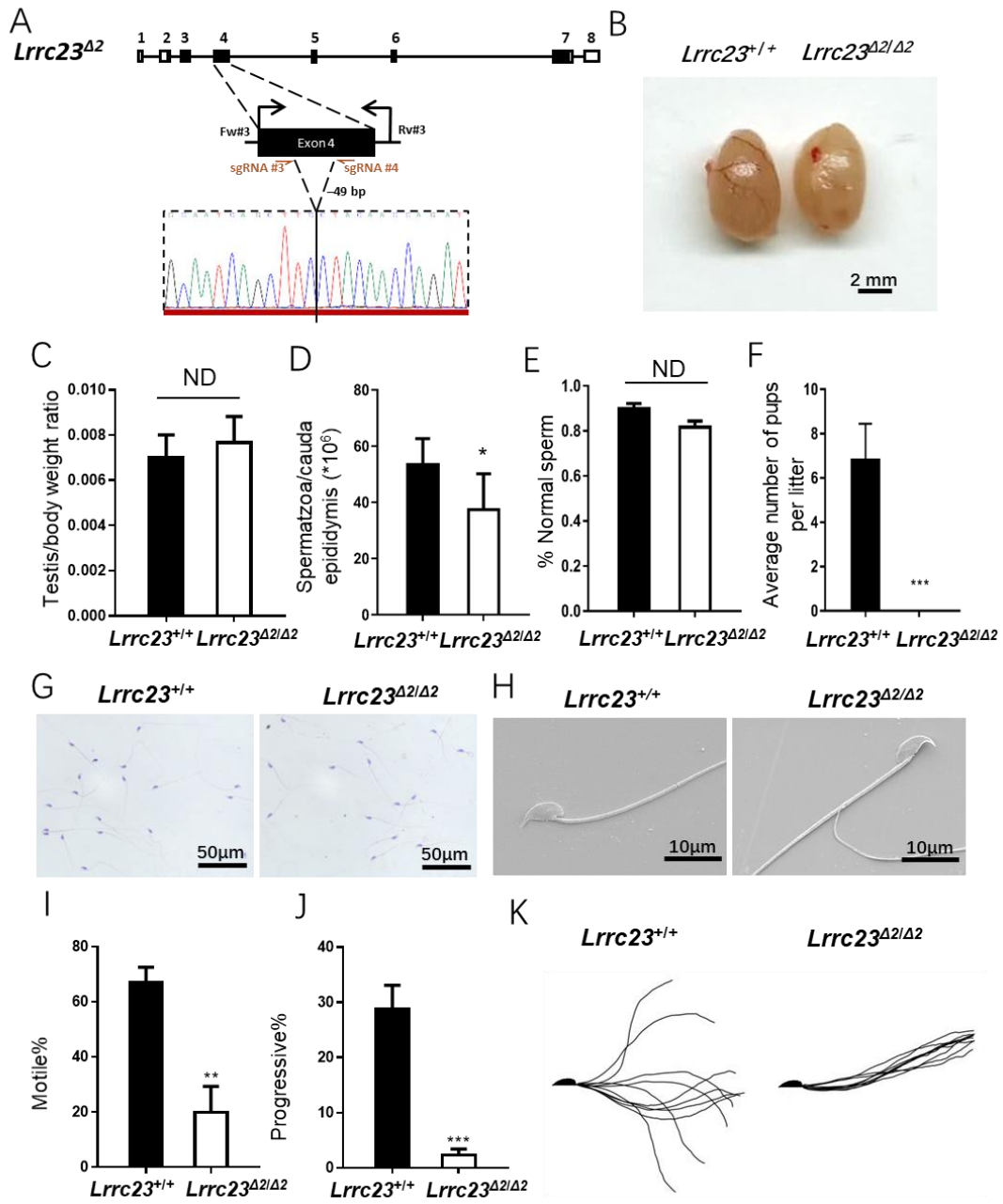


Fig. S3. Generation and analysis of male *Lrrc23*^{A2/A2} mice. (A) Dual sgRNAs (sgRNA#3 and sgRNA#4) were used to target *Lrrc23* exon 4, with Sanger sequencing being used to confirm the successful deletion of a 49 bp fragment within this region. Black rectangles are used to denote the coding regions, and genotyping primers (Fw#3, Rv#3) were as shown. (B) Testes of *Lrrc23*^{+/+} and *Lrrc23*^{A2/A2} mice. (C) Average testis weight/body weight in *Lrrc23*^{+/+} and *Lrrc23*^{A2/A2} mice, N = 3, P > 0.05. Error bars represent S.D. Student's t-test. (D) Cauda epididymal sperm contents from *Lrrc23*^{+/+} and *Lrrc23*^{A2/A2} mice, N = 3, P > 0.05. Error bars represent S.D. Student's t-test. (E) Normal epididymal sperm counts from *Lrrc23*^{+/+} and *Lrrc23*^{A2/A2} mice, N = 3, P > 0.05. Error bars represent S.D. Student's t-test. (F) Average numbers of pups per litter from *Lrrc23*^{+/+} and *Lrrc23*^{A2/A2} mice, N = 3, ***P < 0.001. Error bars represent S.D. Student's t-test. (G) Spermatozoa from *Lrrc23*^{+/+} and *Lrrc23*^{A2/A2} mice were subjected to hematoxylin and eosin staining. (H) SEM was used to image WT and *Lrrc23* knockout spermatozoa. (I) average percentages of motile spermatozoa and (J) progressively motile spermatozoa from *Lrrc23*^{+/+} and *Lrrc23*^{A2/A2} mice were quantified, N = 3, **P < 0.01, ***P < 0.001. Error bars represent S.D. Student's t-test. (K) Flagellar waveforms for spermatozoa from *Lrrc23*^{+/+} and *Lrrc23*^{A2/A2} mice were assessed following a 5 min incubation.

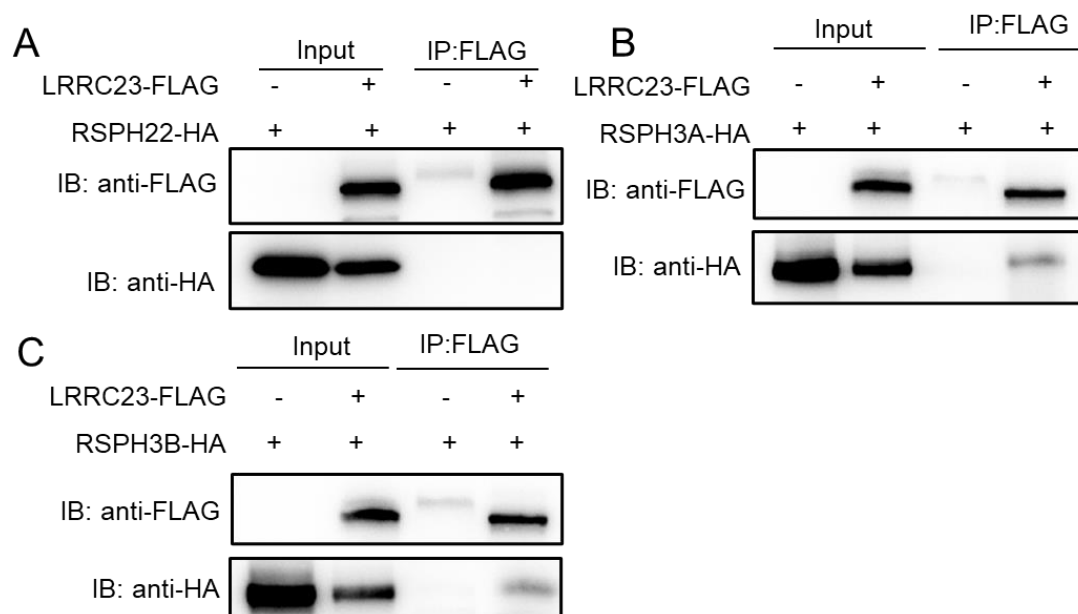
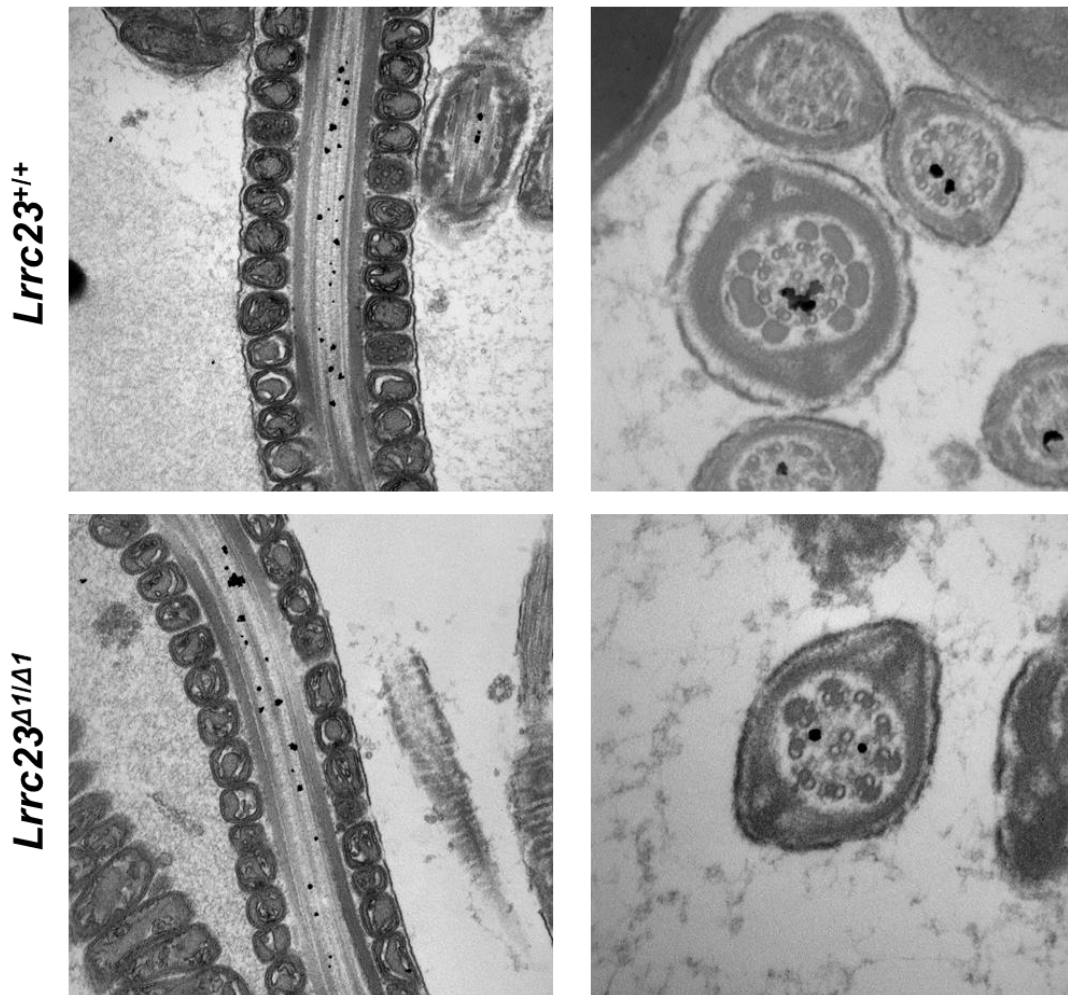


Fig. S4. LRRC23 is a radial spoke complex component that interacts with other proteins within this complex. (A, B and C) Co-immunoprecipitation of LRRC23-FLAG and RSPH-HA was conducted using anti-FLAG-conjugated beads to examine interactions between these two proteins. Input: whole cell lysates from experimental cells; IP: samples immunoprecipitated with anti-FLAG beads. In HEK293T cells, LRRC23 was able to interact with other RS proteins including RSPH22 (A), RSPH3A (B), and RSPH3B (C).

A Localization of RSPH6A in *Lrrc23* WT and KO sperm



B Comparison of RSPH6A and LRRC23 localization in WT sperm

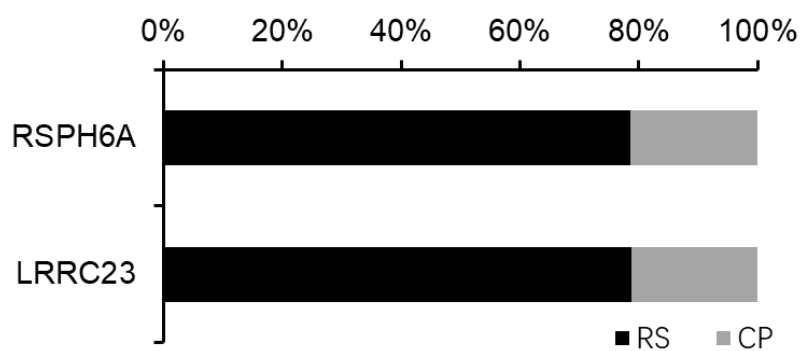


Fig. S5. Analysis of the localization of RSPH6A in the spermatozoa of WT and *Lrrc23*^{Δ1/Δ1} mice by immunoelectron microscopy. (A) RSPH6A antibody-conjugated gold particles were mostly localized to the radial spokes. (B) Comparison of RSPH6A and LRRC23 localization in WT sperm. Both RSPH6A and LRRC23 showed major localization to the radial spokes (RS) and minor localization to the central pair (CP).

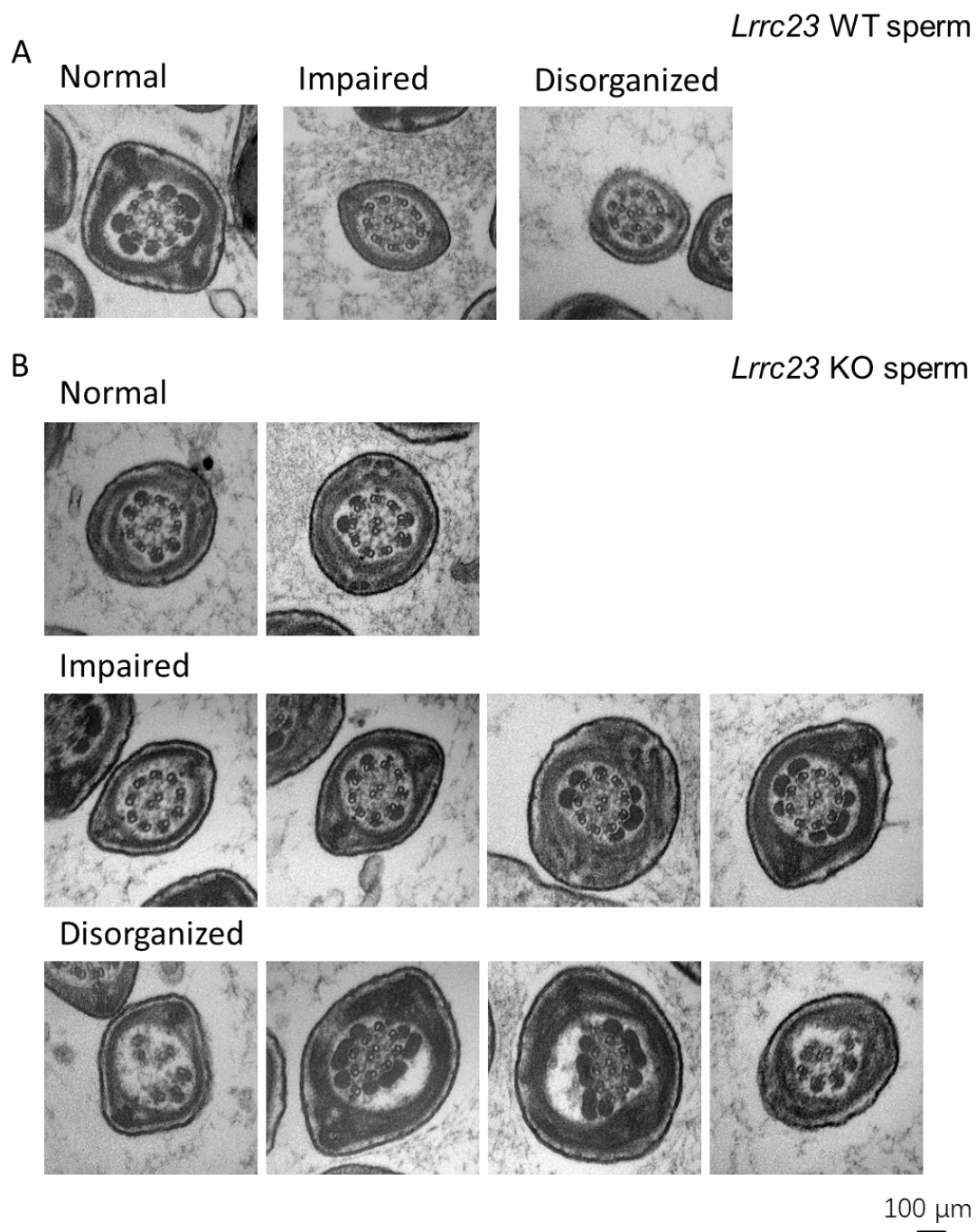


Fig. S6. Ultrastructural analysis of the axonemal structures in WT and *Lrrc23* KO spermatozoa by TEM. (A) Cross sections show normal axonemal structures. (B) Cross sections show unclear RS structures. (C) Cross sections show disorganized microtubule structures.

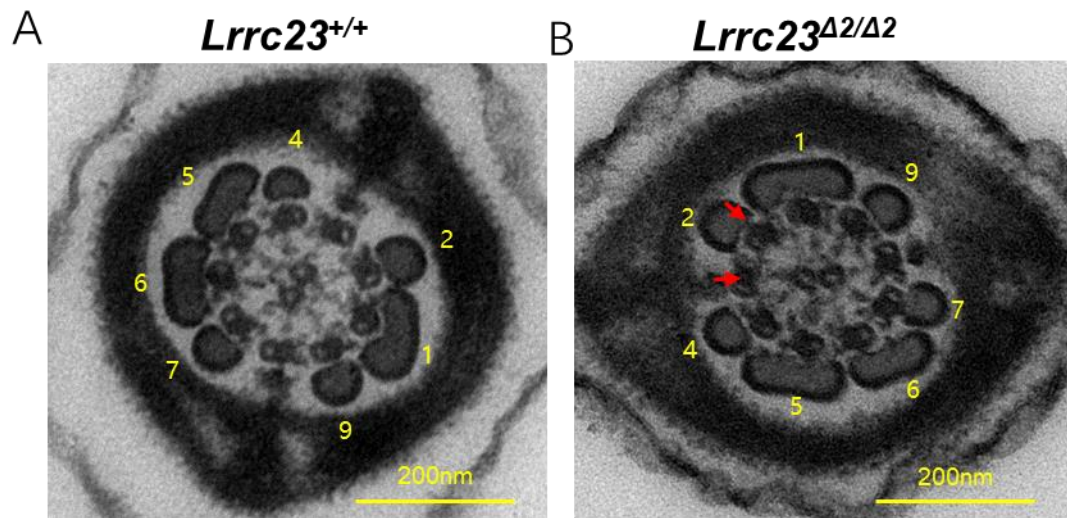


Fig. S7. Ultrastructural assessment of spermatozoa in the cauda epididymis of *Lrrc23*^{Δ2/Δ2} mice. (A and B) Electron microscopy was used to assess cross sections of the principal component of spermatozoa from *Lrrc23*^{+/+} and *Lrrc23*^{Δ2/Δ2} mice. Outer dense fibers are marked with numbers, while the absence of a radial spoke is marked by red arrows.

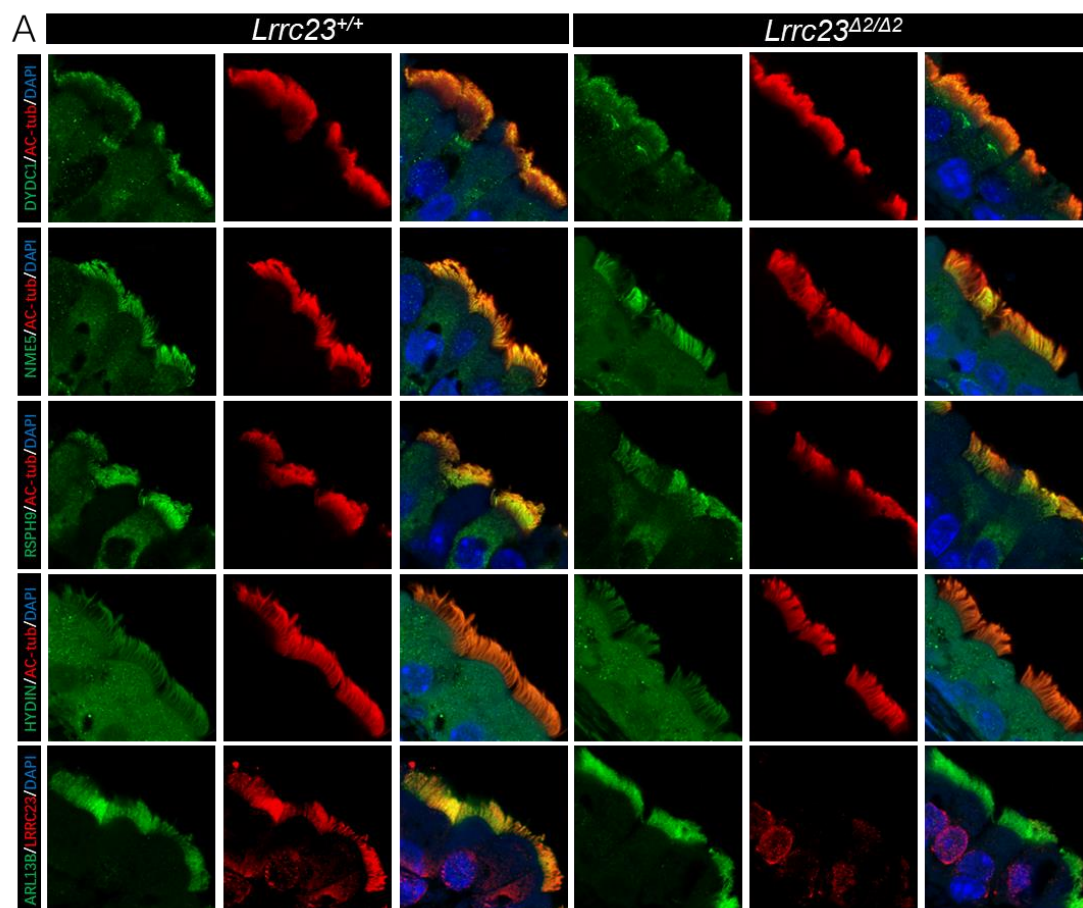


Fig. S8. No significant differences in the tracheal cilia components of *Lrrc23*^{+/+} and *Lrrc23*^{Δ2/Δ2} mice. (A) Immunofluorescent staining of respiratory tract cilia from the indicated mice was performed using antibodies specific for AC-tub, LRRC23 (red), DYDC1, NME5, RSPH9, HYDIN and ARL13B (green). ARL13B regulatory GTPase highly enriched in cilia and used as a marker of cilia. HYDIN is the component of central pairs in motile cilia and flagella. Nuclei were stained with Hoechst 33342 (blue).

Table S1. Primer sequences.

Primer	Sequence
Fw#1:	ACCTGCCCAAACCTTCGAGC
Rv#1:	TGGAGCCTTGTGCATACTAGG
Rv#2:	CCTTCCCACCAGTCGTCTCTA
Fw trans:	GAAATTAATACGACTCACTATAGG
Rv trans:	AAAAGCACCGACTCGGTGCCA
Fw#3:	ACCTCACAGACATCTCCTT
Rv#4:	AACATATACTGCCTGCTTCT
Fw#4:	CCCCTCGAGTTACAGGGCTTTCTTTCCATG
FLAG:	CCCGAATTCGGAGCCGGGAGGAGACCATGT
1D4:	GAATTTATCGTCGTCATCCTTATAATC
RT Fw:	CCAAAAAACAGTCTTGGCG
RT Rv:	CAGACAGATGACTGCCAAGGA

Table S2. List of Antibodies.

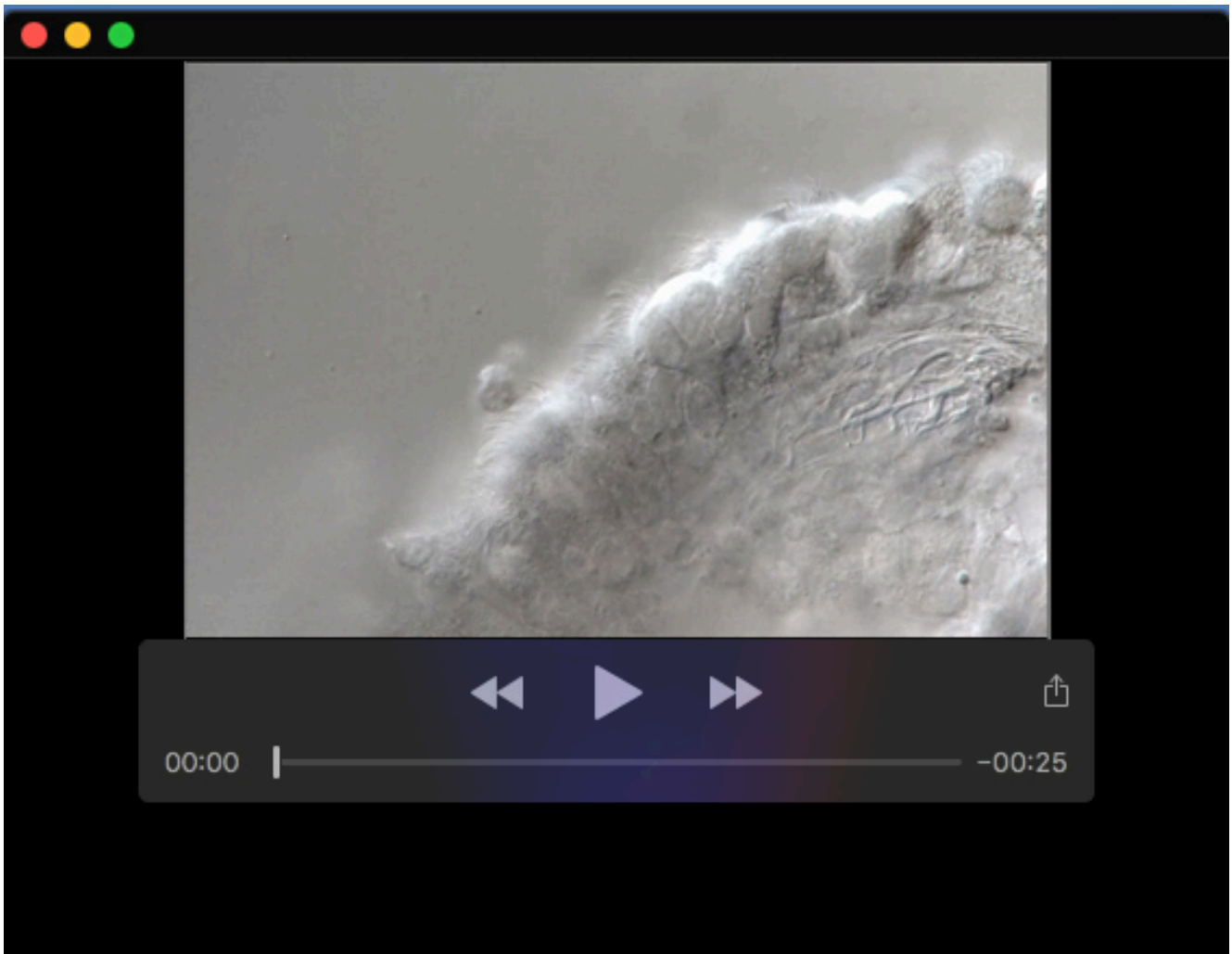
Anitigen	Provider	Catalog number
FALG	MBL	PM020
Acetylated Tubulin	Sigma-Aldrich	T7451
AKAP3	Proteintech	13907-1-AP
HA	MBL	M132-11
AKAP4	BD Biosciences	#611564
DNAH8	Abcam	#ab121989
Beta-Tubulin	Proteintech	10094-1-AP
DRC3	Atlas Antibodies	HPA036040
GAS8	Atlas Antibodies	HPA031703
DYDC1	Proteintech	26327-1-AP
GAPDH	Santa Cruz Biotechnology	#sc-25778
LRRC23	Laboratory of MingXi Liu	
LRRC23	Laboratory of M.I	
RSPH1	Laboratory of M.I	
NME5	Proteintech	12923-1-AP
RSPH4A	Atlas Antibodies	HPA031198
RSPH6A	Laboratory of M.I	
RSPH9	Proteintech	23253-1-AP
RSPH9	Atlas Antibodies	HPA031703
DYNLL2	Proteintech	16811-1-AP
RSPH3	Proteintech	17603-1-AP
SLC2A3	Laboratory of M.I	KS64-10
ARL13B	Proteintech	17711-1-AP
HYDIN	Proteintech	24741-1-AP
Rabbit IgG	CST	2729
Mouse IgG (HRP conjugated)	Jackson ImmunoResearch	115-036-062
Rabbit IgG (HRP conjugated)	Jackson ImmunoResearch	111-036-045
Rat IgG (HRP conjugated)	Jackson ImmunoResearch	112-035-167
Donkey anti-Mouse IgG, Alexa Fluor 488	Invitrogen	A-21202
Donkey anti-Rabbit IgG, Alexa Fluor 488	Invitrogen	A-21206
Donkey anti-Goat IgG, Alexa Fluor 555	Invitrogen	A-21432
Donkey anti-Rabbit IgG, Alexa Fluor 555	Invitrogen	A-31572
Goat anti-Rabbit IgG, HRP	Invitrogen	31460
Goat anti-Mouse IgG, HRP	Invitrogen	31430



Movie S1. Spermatozoa from *Lrrc23^{+Δ1}* mice. Spermatozoa of *Lrrc23^{+Δ1}* mice at 10 min of incubation in TYH media. Movie is recorded at 200 frames/second using an Olympus BX-53 microscope equipped with a high-speed camera (HAS-L1, Ditect, Tokyo, Japan).



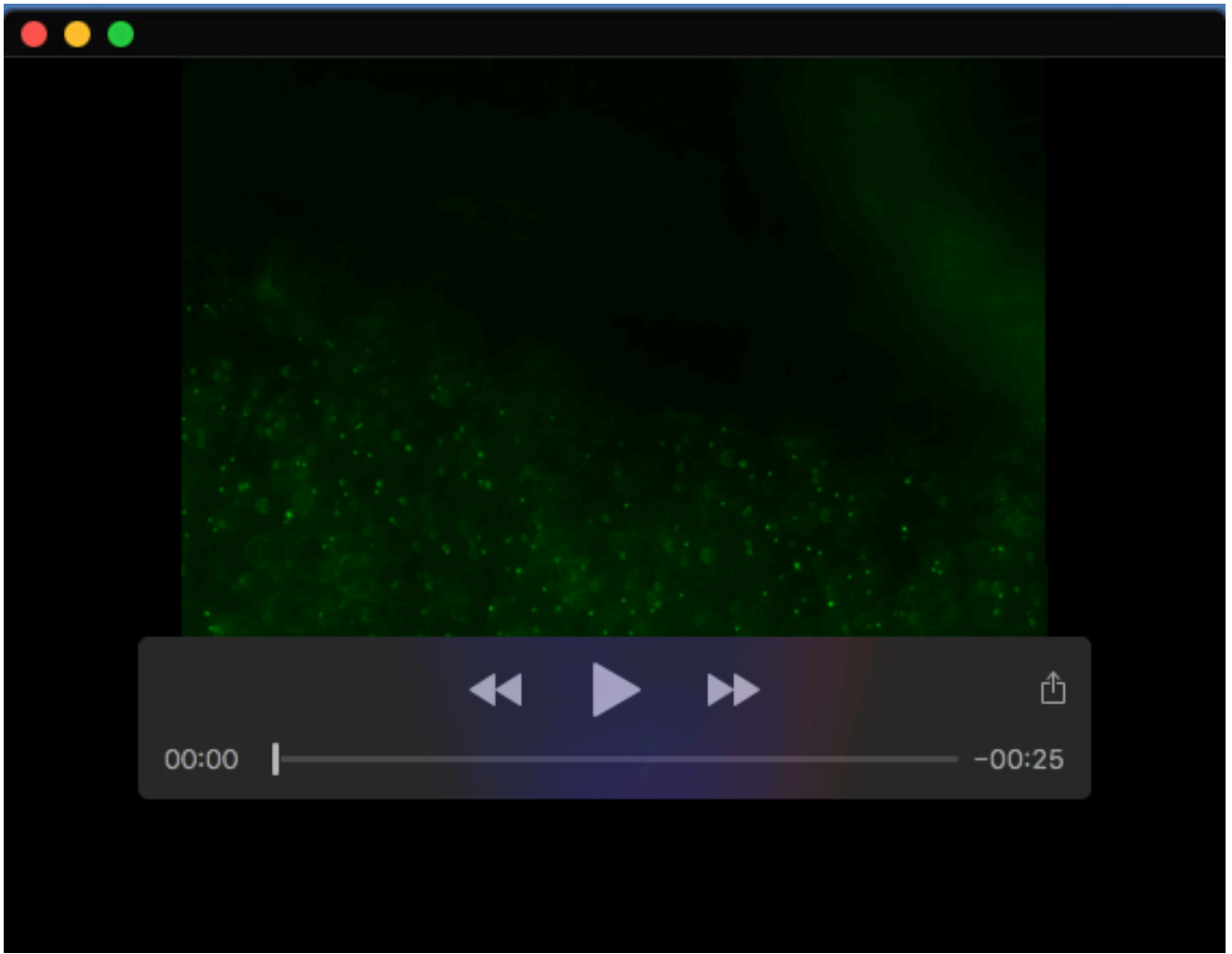
Movie S2. Spermatozoa from *Lrrc23*^{Δ1/Δ1} mice. Spermatozoa of *Lrrc23* knockout mice at 10 min of incubation in TYH media. Movie is recorded at 200 frames/second using an Olympus BX-53 microscope equipped with a high-speed camera (HAS-L1, Ditect, Tokyo, Japan).



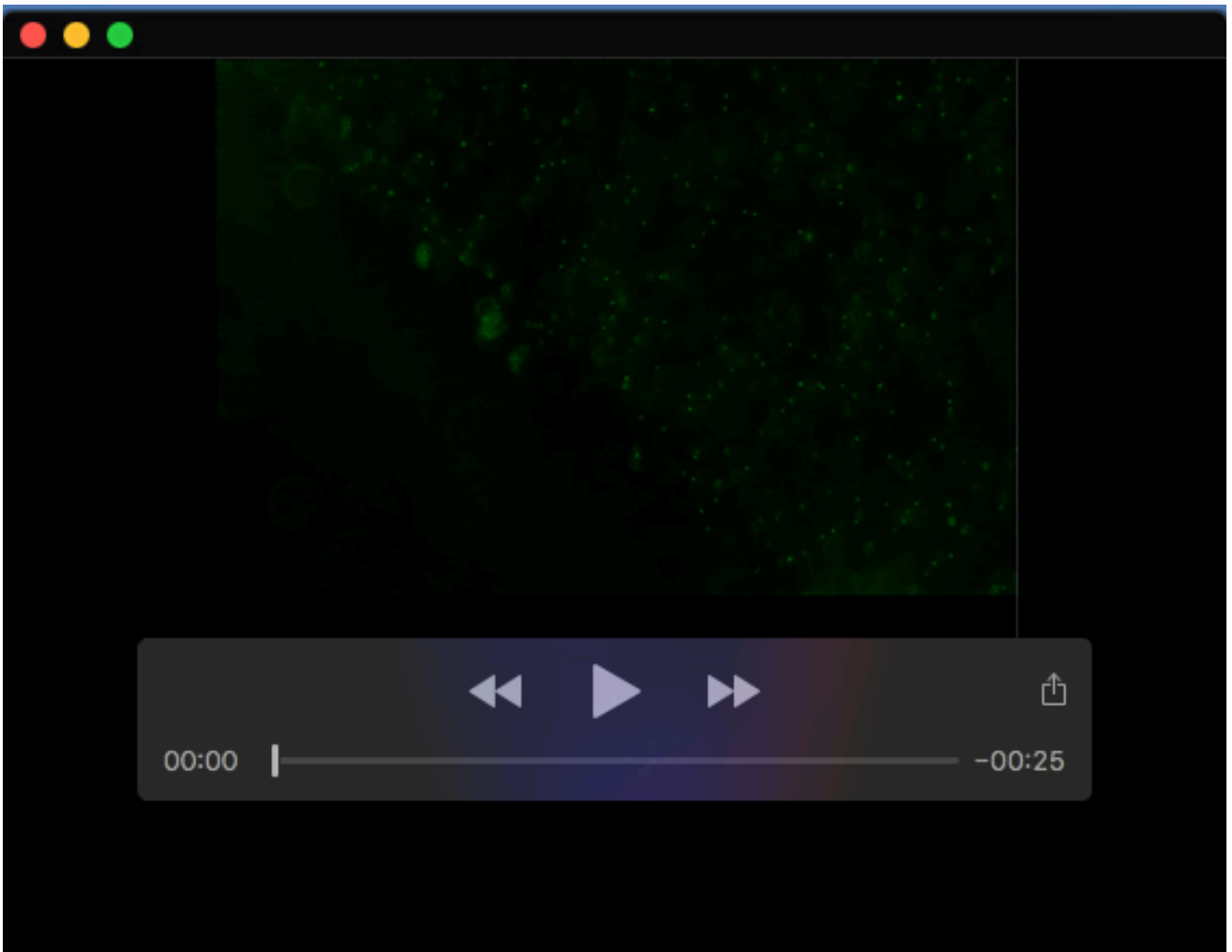
Movie S3. The beating of respiratory cilia in *Lrrc23*^{+/+} mice.



Movie S4. The beating of respiratory cilia in *Lrrc23*^{A2/A2} mice.



Movie S5. Cilia generated flow in *Lrrc23* WT multiciliated tracheal cells.



Movie S6. Cilia generated flow in *Lrrc23* KO multiciliated tracheal cells.